phys. stat. sol. (b) **183**, 529 (1994)

Subject classification: 72.10 and 73.40; 71.25; 72.20; S7.12; S7.15

Department of Physics, University of Science and Technology of China, Hefei[1]) *(a), Department of Physics, Fudan University, Shanghai*[2]) *(b), and Shanghai Institute of Metallurgy, Chinese Academy of Sciences, Shanghai*[3]) *(c)*

Intersubband Coulomb Scattering Effect on High-Field Hot-Electron Transport in a Quantum Wire

By

M. W. Wu (a), Z. G. Yu (b), and X. L. Lei (c)

Hot-electron transport properties of $Al_xGa_{1-x}As/GaAs$ quantum wires under high electric fields are studied by means of the balance-equation approach using a model with multiple species of carriers. Each transverse subband is assumed to have its own electron temperature, Fermi level, and mean drift velocity differing from other nondegenerate subbands. The intersubband Coulomb interactions are taken into account perturbatively for the first time together with acoustic and polar optic phonon scatterings in the numerical calculation. Our calculation shows that although the electron temperatures, Fermi levels, and drift velocities of different subbands differ markedly from each other, the overall average drift velocity and the resultant nonlinear mobility are very close to those predicted by the conventional model assuming single species of carriers in the multisubband quantum wire system.

1. Introduction

Multivalley or multisubband occupations of carriers are known to play an important role in determining their high field transport behavior in bulk [1, 2] and low-dimensional [3 to 8] semiconductors. Electrons in different valleys (subbands) are coupled via electron–phonon, electron–impurity, and electron–electron (e–e) Coulomb interactions. Unlike in a bulk semiconductor, where carriers in different valleys have different effective masses and thus are usually treated as different species of carriers, in a low-dimensional semiconductor system, carriers dwelling in different subbands share a common effective mass and have usually been treated as a single species of carriers. Recently Guillemot et al. [4] studied the electron–longitudinal optical phonon coupling in quasi-two-dimensional quantum wells under steady-state high-field transport conditions. Their calculation, which is based on the balance-equation approach of high-field transport in a two-subband system, assumes a single center-of-mass velocity and a common electron temperature but separate Fermi levels for both subbands. Wang and Lei [7, 8] calculated high-field electron transport in quantum wires assuming a single center-of-mass velocity, a unique electron temperature and a common Fermi level for all the fifteen subbands. The feasibility of these assumptions needs to be examined. In a low-dimensional (e.g. quantum wire) system, although intrasubband Coulomb interaction is believed to be strong in comparison with impurity and phonon scatterings to yield an electron temperature and a Fermi level in each subband, the intersubband Coulomb scatterings, which involve small form factors, may not be strong

[1]) 96, Jingzhai Road, Hefei (Anhui) 230026, People's Republic of China.
[2]) 220, Handan Road, Shanghai 200433, People's Republic of China.
[3]) 865, Changning Road, Shanghai 200050, People's Republic of China.

enough to give a common electron temperature or a common Fermi level for different subbands.

The purpose of this paper is to discuss the Coulomb intersubband scattering on the electron transport in quantum wires using a model with multiple species of carriers. For the sake of simplicity, cylindrical GaAs wires surrounded by AlGaAs are considered where the transverse dimension can be described by one parameter, the radius of the wire which is taken as 9 nm. For this system we can assume that electrons interact only with bulk acoustic (Ac) phonons and longitudinal optical (LO) phonons and calculate the transport properties without impurity scatterings. We consider the electron occupation of the ground and the first excited subbands. Each subband is assumed to have its own electron temperature, Fermi level, and average drift velocity. Our numerical results show that although the electron temperatures, Fermi levels, and the drift velocities of the ground and excited subbands differ markedly from each other, the overall average drift velocity and the resultant nonlinear mobility are very close to those predicted by the conventional model assuming single species of carriers for the multisubband quantum wire system.

2. Hamiltonian and Balance Equations for Forces, Energies, and Particle Numbers

We consider a cylindrical quantum wire of radius ϱ and length L_z, and denote by N the total number of electrons. The electron energy in the quantum wire can be expressed as

$$\varepsilon_n(k_z) = \varepsilon_n + \frac{k_z^2}{2m}, \tag{1}$$

where ε_n is the transverse two-dimensional (2D) energy of the n-th subband, k_z the longitudinal one-dimensional (1D) wave vector, and m the effective mass. To concentrate on the effect of the intersubband Coulomb interaction we consider the electron occupation of the lowest three subbands. The wave functions of these three transverse states are given by

$$\varphi_0 = C_0 \mathrm{J}_0\left(\frac{x_0}{\varrho} r_{\|}\right), \qquad \varphi_{\pm 1} = \pm C_{\pm 1} \mathrm{J}_1\left(\frac{x_1}{\varrho} r_{\|}\right) \mathrm{e}^{\pm i\phi}, \tag{2}$$

where $C_n = (\sqrt{\pi}\, \varrho y_n)^{-1}$ $(n = 0, \pm 1)$ is the normalization factor, $(r_{\|}, \phi)$ denotes the transverse coordinate, $x_{|n|}$ (>0) represents the first zero of the n-th order Bessel function, i.e. $\mathrm{J}_n(x_{|n|}) = 0$ and $y_n = \mathrm{J}_{n+1}(x_{|n|})$. The corresponding eigenenergy is $\varepsilon_n = x_{|n|}^2/(2m\varrho^2)$. It is easy to see that the $n = 1$ subband is degenerate with the $n = -1$ one. In the following, we label these two degenerate states as 1 and -1, respectively, and the ground state as 0.

In the framework of balance-equation approach [9, 10], the Hamiltonian of the system is written in the form

$$H = H_{\mathrm{c}} + H_{\mathrm{e}} + H_{\mathrm{p}} + H_{\mathrm{ep}}, \tag{3}$$

where

$$H_{\mathrm{c}} = H_{0\mathrm{c}} + H_{1\mathrm{c}} + H_{-1\mathrm{c}},$$

$$H_{0\mathrm{c}} = \tfrac{1}{2} m\hat{N}_0 v_0^2 - \hat{N}_0 E Z_0,$$

$$H_{\pm 1\mathrm{c}} = \tfrac{1}{2} m\hat{N}_{\pm 1} v_{\pm 1}^2 - \hat{N}_{\pm 1} E Z_{\pm 1}$$

are the center-of-mass (CM) Hamiltonians, where v_i and Z_i are the CM drift velocity and coordinate (in z-direction) of subband i ($i = 0, \pm 1$). $\boldsymbol{E} = E\hat{\boldsymbol{z}}$ is the applied electric field along the wire. $\hat{N}_0$, $\hat{N}_1$, and $\hat{N}_{-1}$ are the electron numbers of subbands 0, 1, and -1. In the second quantization representation of the relative electron systems they are expressed by ($n = 0, \pm 1$)

$$\hat{N}_n = \sum_{k_z\sigma} c^{\dagger}_{nk_z\sigma} c_{nk_z\sigma} , \tag{4}$$

$N_0 + N_1 + N_{-1} = N$. We assume, for the two degenerate subbands 1 and -1, that the average velocities and electron numbers are equal, $v_{1d} = v_{-1d}$, and $N_1 = N_{-1}$. The relative electron Hamiltonian reads

$$H_e = \sum_{nk_z\sigma} \varepsilon_n(k_z)\, c^{\dagger}_{nk_z\sigma} c_{nk_z\sigma} + \sum_{nn'mm'} \sum_{k_z k'_z q_z} \sum_{\sigma\sigma'} K_{nn',\,m'm}(|q_z|)\, c^{\dagger}_{nk_z+q_z\sigma} c^{\dagger}_{n'k'_z-q_z\sigma'} c_{m'k'_z\sigma'} c_{mk_z\sigma} . \tag{5}$$

$$K_{nn',\,m'm}(|q_z|) = \frac{e^2}{4\pi\epsilon_0 \varkappa L_z} \int \mathrm{d}\boldsymbol{r}_{\parallel}\, \mathrm{d}\boldsymbol{r}'_{\parallel}\, \varphi^*_n(\boldsymbol{r}_{\parallel})\, \varphi^*_{n'}(\boldsymbol{r}'_{\parallel})\, \varphi_{m'}(\boldsymbol{r}'_{\parallel})\, \varphi_m(\boldsymbol{r}_{\parallel})\, \mathrm{K}_0(|q_z|\, |\boldsymbol{r}_{\parallel} - \boldsymbol{r}'_{\parallel}|) \tag{6}$$

is the Coulomb interaction and $\varkappa$ the low-frequency dielectric constant. $\mathrm{K}_0(x)$ is the modified Bessel function of zeroth order.

$$H_p = \sum_{\boldsymbol{q}\lambda} \Omega_{\boldsymbol{q}\lambda} b^{\dagger}_{\boldsymbol{q}\lambda} b_{\boldsymbol{q}\lambda} \tag{7}$$

is the Hamiltonian of bulk phonons; $\boldsymbol{q} = (\boldsymbol{q}_{\parallel}, q_z)$.

$$H_{ep} = \sum_{nn'} \sum_{\boldsymbol{q}\lambda} \sum_{\sigma} M(n, n', \boldsymbol{q}, \lambda)\, (b_{\boldsymbol{q}\lambda} + b^{\dagger}_{-\boldsymbol{q}\lambda})\, c^{\dagger}_{nk_z+q_z\sigma} c_{n'k_z\sigma} \tag{8}$$

is the coupling between electrons and bulk phonons, the coupling matrix element is

$$M(n, n', \boldsymbol{q}, \lambda) = M(\boldsymbol{q}, \lambda)\, F_{nn'}(q_{\parallel})$$

with the 3D electron–phonon coupling matrix element $M(\boldsymbol{q}, \lambda)$, and the form factor is given by

$$F_{nn'}(q_{\parallel}) = 2 \int_0^1 \xi\, \mathrm{d}\xi\, \frac{1}{y_n y'_n}\, \mathrm{J}_n(x_{|n|}\xi)\, \mathrm{J}_{n'}(x_{|n'|}\xi)\, \mathrm{J}_{|n-n'|}(q_{\parallel}\varrho\xi) . \tag{9}$$

The intrasubband form factors F_{00} and F_{11} and intersubband form factors F_{01} and F_{1-1} are illustrated in Fig. 1. The $K_{nn',\,m'm}$ term in the electron–electron Coulomb interaction describes the collision between an electron in subband m and an electron in subband m', which are scattered, respectively, into subband n and subband n'. $K_{00,\,00}$, $K_{11,\,11}$, and $K_{-1-1,\,-1-1}$ are involved in pure intrasubband Coulomb scattering. These collisions contribute to establishing an electron temperature within each subband. In our treatment, we have assumed that each subband has its own temperature and hence we need not calculate the explicit expressions of $K_{00,\,00}$, $K_{11,\,11}$, and $K_{-1-1,\,-1-1}$. Furthermore, the two degenerate subbands 1 and -1 are assumed to share a common electron temperature and there is no need for the explicit expressions of intersubband Coulomb scattering between these two subbands. The collisions between electrons in the ground subband 0 and electrons in the first excited subbands 1 and -1 are essential in our model. As a matter of fact there

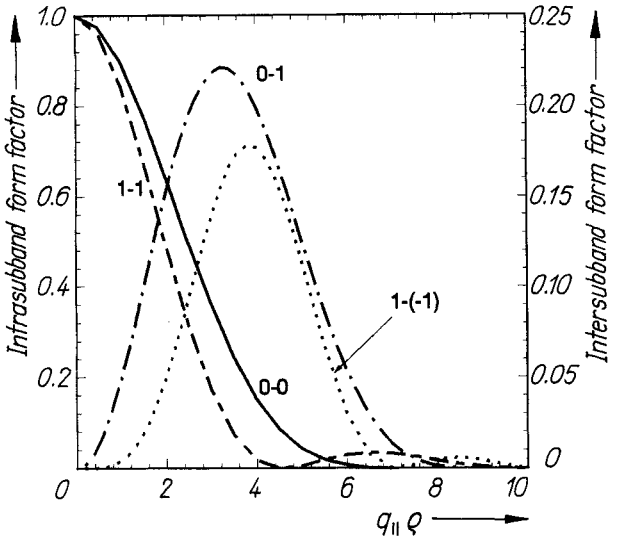

Fig. 1. Intrasubband (0–0 and 1–1) and intersubband (0–1 and 1–(−1)) form factors as functions of normalized transverse wave vector $q_{\|}\varrho$

are only two classes of nonzero coefficients in our model. The first class including $K_{01,10} = K_{0-1,-10} = K_{10,01} = K_{-10,0-1} \equiv v\mathscr{K}(|q_z|)$, describes collisions between two electrons of different subbands but which are scattered within the same subband. This kind of collisions tends to give a common temperature for the ground subband and the first excited subbands. $v = e^2/(4\pi\epsilon_0\varkappa L_z)$. The second class, including $K_{01,01}$, $K_{10,10}$, $K_{0-1,0-1}$, $K_{-10,-10}$, $K_{1-1,00}$, $K_{-11,00}$, $K_{00,1-1}$, and $K_{00,-11}$ involves exchange of particles between different subbands with conserving the number of electrons within each subband ($K_{01,01}$, $K_{10,10}$, $K_{0-1,0-1}$, and $K_{-10,-10}$) or with transferring two electrons from one subband to the other ($K_{1-1,00}$, $K_{-11,00}$, $K_{00,1-1}$, and $K_{00,-11}$). All these coefficients have the same value and will be denoted by $v\mathscr{K}'(|q_z|)$ in the following. In Fig. 2 $\mathscr{K}^2$ and $\mathscr{K}'^2$ are plotted as functions of $|q_z|\,\varrho$. Note that $\mathscr{K}^2$ is almost two orders of magnitude larger than $\mathscr{K}'^2$. Hence the Coulomb interaction can be separated into three parts: the first is the "intrasubband" part containing $K_{nn,nn}$ (with $n = 0, \pm 1$), which contribute to an electron temperature T_{ne} in subband n. The second part includes terms $K_{nn',mm'}$ (with n, n', m, $m' = \pm 1$), which is assumed to be efficient in rendering $T_{1e} = T_{-1e}$. The last part, which is made up of the remaining terms, will be denoted by H_e^1. The relative electron Hamiltonian can now be rewritten as $H_e = H_{0e} + H_{\pm 1e} + H_e^1$, in which

$$H_{0e} = \sum_{k_z\sigma} \varepsilon_0(k_z)\, c^\dagger_{0k_z\sigma} c_{0k_z\sigma} + \sum_{k_z k_z' q_z} \sum_{\sigma\sigma'} K_{00,00}(|q_z|)\, c^\dagger_{0,k_z+q_z\sigma} c_{0,k_z'-q_z\sigma'} c_{0k_z'\sigma'} c_{0k_z\sigma}\,,$$

$$H_{\pm 1e} = \sum_{k_z\sigma} \sum_{n=\pm 1} \varepsilon_n(k_z)\, c^\dagger_{nk_z\sigma} c_{nk_z\sigma} + \sum_{nn'mm'=\pm 1} \sum_{k_z k_z' q_z} \sum_{\sigma\sigma'} K_{nn',m'm}(|q_z|)\, c^\dagger_{n,k_z+q_z\sigma} c_{n',k_z'-q_z\sigma'} c_{m',k_z'\sigma'} c_{mk_z\sigma}\,.$$

H_e^1, along with electron–phonon interaction H_{ep}, will be handled perturbatively against $H_0 = H_{0e} + H_{\pm 1e} + H_p$. In the balance-equation theories [9]

$$\hat{\varrho}_0 = \frac{1}{Z} \exp(-H_{0e}/T_{0e}) \exp(-H_{\pm 1e}/T_{1e}) \exp(H_p/T) \tag{10}$$

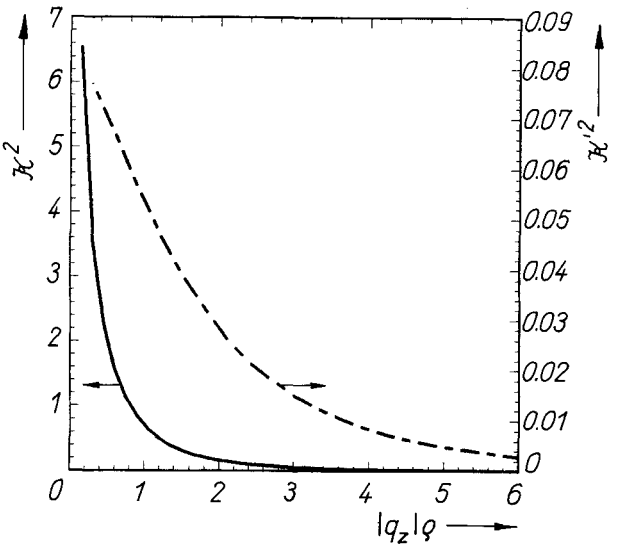

Fig. 2. Intersubband Coulomb "form factors" $\mathcal{K}^2$ (solid curve) and $\mathcal{K}'^2$ (dash-dotted curve) as functions of normalized 1D wave vector $|q_z|\,\varrho$

with T being the lattice temperature. The density matrix $\hat{\varrho}(t)$ should satisfy the Liouville equation $i\,\mathrm{d}\hat{\varrho}(t)/\mathrm{d}t = [H, \hat{\varrho}(t)]$ and the initial condition $\hat{\varrho}(t_0) = \hat{\varrho}_0$. The statistical averages of the rate of change of the electron total momentum $P_n = N_n m v_{nd}$ $(n = 0, \pm 1)$, $\dot{P}_n = -i[P_n, H]$, the rate of change of the electron energy, $\dot{H}_{ne} = -i[H_{ne}, H]$ in subband n, and the rate of change of the particle number, $\dot{\hat{N}}_0 = -i[\hat{N}_0, H]$, in a steady-transport state, lead to the force, energy, and particle number balance equations,

$$\frac{1}{N} N_0 eE + F_{0p} + F_{0c} = 0\,, \tag{11}$$

$$\frac{2N_1}{N} eE + F_{1p} + F_{-1p} + F_{1c} + F_{-1c} = 0\,, \tag{12}$$

$$-\frac{N_0}{N} e v_{0d} E + W_{0p} + W_{0c} = 0\,, \tag{13}$$

$$-\frac{2N_1}{N} e v_{1d} E + W_{1p} + W_{-1p} + W_{1c} + W_{-1c} = 0\,, \tag{14}$$

$$\mathcal{N}(v_{0d}, v_{1d}, T_{0e}, T_{1e}, \mu_{0F}, \mu_{1F}) = 0\,. \tag{15}$$

These five equations, together with the constraint

$$N_0 + 2N_1 = N \tag{16}$$

and the relations

$$N_n = \sum_{k_z \sigma} f([\varepsilon_n(k_z) - \mu_{nF}]/T_{ne}) \quad (n = 0, 1) \tag{17}$$

($f(x) = 1/[\exp(x) + 1]$ is the Fermi function) form a complete set of equations to determine the steady-state values of v_{0d}, v_{1d}, T_{0e}, T_{1e}, μ_{0F}, μ_{1F}, N_0, and N_1 at given E, T, and N. The expressions for F_{np}, F_{nc}, W_{np}, W_{nc} $(n = 0, \pm 1)$, and $\mathcal{N}$ in (11) to (15) are given in the Appendix.

Table 1
Parameters used in the numerical calculations

$\varkappa_\infty$	10.8	$\varkappa$	12.9
Ω_0 (meV)	35.4	Ξ (eV)	7
m/m_e	0.07	N_e (m^{-3})	8.35×10^{23}
v_{sl} (m/s)	5.3×10^3	d (kg/m^3)	5.3×10^3

3. Numerical Results and Discussion

We have performed numerical calculations from (11) to (17) of the two-species-of-carriers model (TSCM) for an $Al_xGa_{1-x}As/GaAs$ quantum wire to obtain high-field steady-state transport for electric fields up to 10^5 V/m at lattice temperature $T = 100$ K. In the calculation we have included all the intrasubband and intersubband scatterings due to LO phonons with the Fröhlich matrix element

$$|M(q, \mathrm{LO})|^2 = \frac{e^2}{2\pi\varrho^2 L_z \epsilon_0 q^2}\left(\frac{1}{\varkappa_\infty} - \frac{1}{\varkappa}\right)\Omega_0 ,$$

and those due to Ac phonons with the deformation potential matrix element

$$|M(q, \mathrm{Ac})|^2 = \frac{\Xi^2 q}{2\pi\varrho^2 L_z \, \mathrm{d}v_{sl}} .$$

Here $\varkappa_\infty$ is the optical dielectric constant, Ω_0 the LO-phonon frequency, Ξ the acoustic phonon deformation potential, v_{sl} the longitudinal sound velocity, and d the mass density of the crystal. The values of these parameters are given in Table 1.

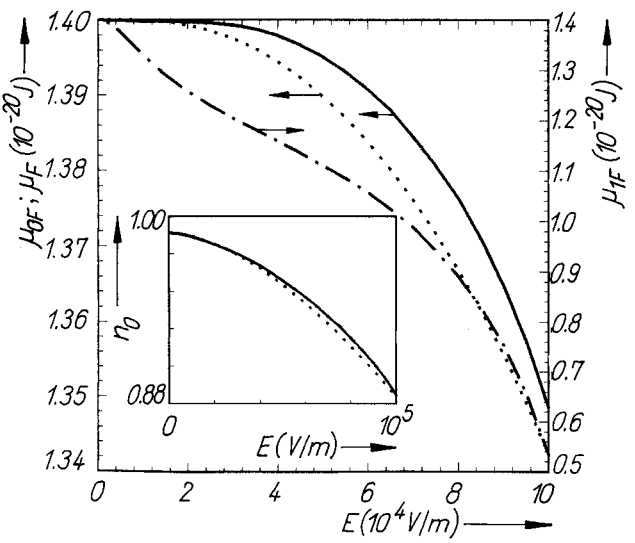

Fig. 3. Calculated Fermi level vs. electric field E. The solid and dash-dotted curves are, respectively, μ_{0F} and μ_{1F} predicted by TSCM. The dotted curve is the calculated result of μ_F from SSCM. The inset shows the fraction of electrons in subband 0 predicted by TSCM (solid curve) and by SSCM (dotted curve)

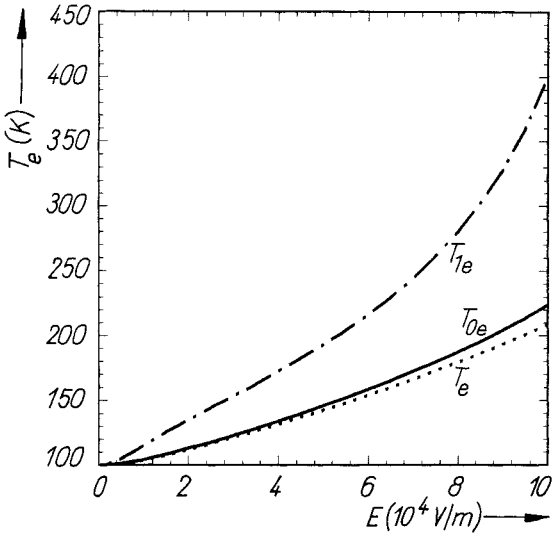

Fig. 4. The electron temperature as a function of external electric field E. The solid curve represents T_{0e}, the electron temperature of subband 0, and the dash-dotted curve stands for T_{1e}, the electron temperature of subband 1 (and -1) obtained in TSCM. The dotted curve is the electron temperature T_e, obtained by SSCM

For comparison we have also performed numerical calculations for the same system using the single-species-of-carriers model (SSCM), i.e. assuming a common center-of-mass velocity v_d, a single electron temperature T_e, and a unique Fermi level μ_F for all the electrons in different subbands as in [7, 8].

In Fig. 3 we plot the calculated Fermi levels as functions of the applied electric field E. In absence of the applied field E, $\mu_{0F} = \mu_{1F}$ and they split off when $E \neq 0$. The inset of the figure shows the fraction of electrons in the ground subband: $n_0 \equiv N_0/N$. The solid and dash-dotted curves are the results of TSCM and the dotted curves are results of SSCM. The two models predict different Fermi levels and electron occupations.

In TSCM the electron temperatures of the ground subband (T_{0e}) and the upper ones (T_{1e}) differ markedly at high fields as shown in Fig. 4. The electrons in the upper subbands are hotter than those in the ground one. The electron temperature T_e predicted by SSCM is very close to but slightly lower than T_{0e}. This tallies with the electron occupations n_0 predicted by the two models as shown in Fig. 4.

The drift velocities v_{0d} and v_{1d} calculated from TSCM are plotted in Fig. 5 as functions of the applied electric field. The overall averaged drift velocity

$$\bar{v}_d = \frac{N_0 v_{0d} + 2N_1 v_{1d}}{N} \tag{18}$$

and the nonlinear mobility

$$\bar{\mu} = \frac{\bar{v}_d}{E} \tag{19}$$

predicted by TSCM, and the drift velocity v_d and nonlinear mobility μ obtained in SSCM, are also shown in the figure. It can be seen from the figure that although the drift velocity v_{1d} of the upper subbands is markedly higher than that of the ground subband, v_{0d} in TSCM, the overall average drift velocity $\bar{v}_d$ and nonlinear mobility $\bar{\mu}$ predicted by TSCM

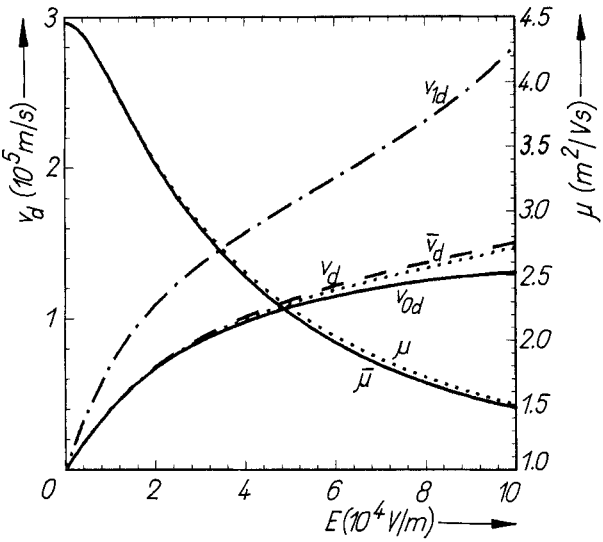

Fig. 5. Steady-state drift velocities v_{0d} and v_{1d} of subbands 0 and 1(−1) and the overall average drift velocity $\bar{v}_d$ and nonlinear mobility $\bar{\mu}$ calculated by TSCM, are shown as functions of the applied electric field E. For comparison, the steady-state drift velocity v_d and nonlinear mobility μ, predicted by SSCM for the same GaAs quantum wire are also shown

are very close to v_d and μ obtained in SSCM. This justifies that the much more simplified SSCM calculation yields essentially correct results for the overall drift velocity and nonlinear mobility in a realistic quantum wire system.

Acknowledgements

The authors thank the National Natural Science Foundation of China for the support of this work. One of the authors (M. W. W.) would like to thank Prof. L. Z. Cao for the invaluable support for his work.

Appendix

We give below the full expressions of the quantities appeared in the balance equations (11 to 15). The forces and the energy loss rates induced by LO and Ac phonons are given by

$$F_{0p} = 2\sum_{\boldsymbol{q}\lambda} |M(0,0,\boldsymbol{q},\lambda)|^2 \, q_z \Pi_2(0,0,q_z,\Omega_{\boldsymbol{q}\lambda}+\omega_0) \times\left[n\left(\frac{\Omega_{\boldsymbol{q}\lambda}}{T}\right) - n\left(\frac{\Omega_{\boldsymbol{q}\lambda}+\omega_0}{T_{0e}}\right)\right] + 2f_{0p}\,, \tag{A1}$$

$$f_{0p} = -4\pi \sum_{k_z\boldsymbol{q}\lambda} |M(0,1,\boldsymbol{q},\lambda)|^2 \, k_z[f(\xi_{0k_z}/T_{0e}) - f(\xi_{1k_z+q_z}/T_{1e})] \times\left\{\left[n\left(\frac{\Omega_{\boldsymbol{q}\lambda}}{T}\right) - n\left(\frac{\xi_{0k_z}}{T_{0e}} - \frac{\xi_{1k_z+q_z}}{T_{1e}}\right)\right]\delta(E_{1k_z+q_z} - E_{0k_z} + \Omega_{\boldsymbol{q}\lambda}) + \left[n\left(\frac{\Omega_{\boldsymbol{q}\lambda}}{T}\right) - n\left(\frac{\xi_{1k_z+q_z}}{T_{1e}} - \frac{\xi_{0k_z}}{T_{0e}}\right)\right]\delta(E_{1k_z+q_z} - E_{0k_z} - \Omega_{\boldsymbol{q}\lambda})\right\}, \tag{A2}$$

$$F_{1p} + F_{-1p} = 2 \sum_{n,m=\pm 1} \sum_{q\lambda} |M(n, m, q, \lambda)|^2 \, q_z \Pi_2(m, n, q_z, \Omega_{q\lambda} + \omega_1) \times \left[n\left(\frac{\Omega_{q\lambda}}{T}\right) - n\left(\frac{\Omega_{q\lambda} + \omega_1}{T_{1e}}\right)\right] + 2f_{1p}, \tag{A3}$$

$$W_{0p} = 2 \sum_{q\lambda} |M(0, 0, q, \lambda)|^2 \, \Omega_{q\lambda} \Pi_2(0, 0, q_z, \Omega_{q\lambda} + \omega_0) \times \left[n\left(\frac{\Omega_{q\lambda}}{T}\right) - n\left(\frac{\Omega_{q\lambda} + \omega_0}{T_{0e}}\right)\right] + 2w_{0p}, \tag{A4}$$

$$w_{0p} = -4\pi \sum_{k_z q\lambda} |M(0, 1, q, \lambda)|^2 \, \varepsilon_0(k_z) [f(\xi_{0k_z}/T_{0e}) - f(\xi_{1k_z+q_z}/T_{1e})] \times \left\{ \left[n\left(\frac{\Omega_{q\lambda}}{T}\right) - n\left(\frac{\xi_{0k_z}}{T_{0e}} - \frac{\xi_{1k_z+q_z}}{T_{1e}}\right)\right] \delta(E_{1k_z+q_z} - E_{0k_z} + \Omega_{q\lambda}) + \left[n\left(\frac{\Omega_{q\lambda}}{T}\right) - n\left(\frac{\xi_{1k_z+q_z}}{T_{1e}} - \frac{\xi_{0k_z}}{T_{0e}}\right)\right] \delta(E_{1k_z+q_z} - E_{0k_z} - \Omega_{q\lambda}) \right\}, \tag{A5}$$

$$W_{1p} + W_{-1p} = 2 \sum_{n,m=\pm 1} \sum_{q\lambda} |M(n, m, q, \lambda)|^2 \, \Omega_{q\lambda} \Pi_2(m, n, q_z, \Omega_{q\lambda} + \omega_1) \times \left[n\left(\frac{\Omega_{q\lambda}}{T}\right) - n\left(\frac{\Omega_{q\lambda} + \omega_1}{T_{1e}}\right)\right] + 2w_{1p} \tag{A6}$$

with $\omega_n = v_{nd} q_z$, $\xi_{nk_z} = \varepsilon_n(k_z) - \mu_{nF}$ and $E_{nk_z} = \varepsilon_n(k_z) + k_z v_{nd}$ ($n = 0, 1$). $\Pi_2(n, n', q_z, \omega)$ is the imaginary part of the e–e correlation function $\Pi(n, n', q_z, \omega)$. In the absence of dynamic screening, it takes the form

$$\Pi_0(n, n', q_z, \omega) = 2 \sum_{k_z} \frac{f(\varepsilon_n(k_z)) - f(\varepsilon_{n'}(k_z + q_z))}{\omega + \varepsilon_n(k_z) + \varepsilon_{n'}(k_z + q_z) + i\delta}. \tag{A7}$$

The expressions for f_{1p} and w_{1p} can be obtained from (A2) and (A5), respectively by exchanging all the indices $0 \leftrightarrow 1$.

The force experienced by the center of mass and the energy-loss rate of electrons in subband 0 due to intersubband Coulomb interaction, are

$$F_{0c} = 2 \sum_{q_z} |\mathscr{K}(|q_z|)|^2 \, v^2 q_z \int_{-\infty}^{\infty} \frac{d\omega}{\pi} \left[n\left(\frac{\omega}{T_{0e}}\right) - n\left(\frac{\omega - \omega_{01}}{T_{1e}}\right)\right] \times \Pi_2(0, 0, q_z, \omega) \, \Pi_2(1, 1, q_z, \omega - \omega_{01}), \tag{A8}$$

$$W_{0c} = 2 \sum_{q_z} |\mathscr{K}(|q_z|)|^2 \, v^2 \int_{-\infty}^{\infty} \frac{d\omega}{\pi} \omega \left[n\left(\frac{\omega}{T_{0e}}\right) - n\left(\frac{\omega - \omega_{01}}{T_{1e}}\right)\right] \times \Pi_2(0, 0, q_z, \omega) \, \Pi_2(1, 1, q_z, \omega - \omega_{01}), \tag{A9}$$

in which $\omega_{01} = \omega_0 - \omega_1 = q_z(v_{0d} - v_{1d})$. The forces and the energy-loss rate of electrons in subbands 1 and -1 due to intersubband Coulomb interaction $F_{1c} + F_{-1c}$ and $W_{1c} + W_{-1c}$ can be obtained from (A8) and (A9), respectively, by exchanging all the indices $0 \leftrightarrow 1$.

Finally, the rate of change of the electron number of the ground subband reads

$$\begin{aligned}
&\mathcal{N}(v_{0d}, v_{1d}, T_{0e}, T_{1e}, \mu_{0F}, \mu_{1F}) \\
&= -8\pi \sum_{k_z q \lambda} |M(0, 1, \boldsymbol{q}, \lambda)|^2 [f(\xi_{0k_z}/T_{0e}) - f(\xi_{1k_z+q_z}/T_{1e})] \\
&\quad \times \left\{ \left[n\left(\frac{\Omega_{q\lambda}}{T}\right) - n\left(\frac{\xi_{0k_z}}{T_{0e}} - \frac{\xi_{1k_z+q_z}}{T_{1e}}\right) \right] \delta(E_{1k_z+q_z} - E_{0k_z} + \Omega_{q\lambda}) \right. \\
&\quad \left. + \left[n\left(\frac{\Omega_{q\lambda}}{T}\right) - n\left(\frac{\xi_{1k_z+q_z}}{T_{1e}} - \frac{\xi_{0k_z}}{T_{0e}}\right) \right] \delta(E_{1k_z+q_z} - E_{0k_z} - \Omega_{q\lambda}) \right\}. \qquad \text{(A10)}
\end{aligned}$$

References

[1] J. B. GUNN, Solid State Commun. **1**, 88 (1963).
[2] X. L. LEI, D. Y. XING, M. LIU, C. S. TING, and J. L. BIRMAN, Phys. Rev. B **36**, 9134 (1987).
[3] C. GUILLEMOT, F. CLÉROT, P. AUVRY, M. BAUDET, M. GAUNEAU, and A. REGRENY, Semicond. Sci. Technol. **4**, 1142 (1989).
[4] C. GUILLEMOT, F. CLÉROT, and A. REGRENY, Phys. Rev. B **46**, 10152 (1992).
[5] T. YAMADA and J. SONE, Phys. Rev. B **40**, 6265 (1989).
[6] K. W. KIM, M. A. STROSCIO, A. BHATT, R. MICKEVICIUS, and V. V. MITIN, J. appl. Phys. **70**, 319 (1991).
[7] X. F. WANG and X. L. LEI, phys. stat. sol. (b) **175**, 433 (1993).
[8] X. F. WANG and X. L. LEI, Phys. Rev. B **47**, 16612 (1993).
[9] X. L. LEI and C. S. TING, Phys. Rev. B **30**, 4809 (1984); **32**, 1112 (1985).
[10] X. L. LEI and N. J. M. HORING, Internat. J. mod. Phys. B **6**, 805 (1992).

(Received January 19, 1994)